

Self-collimated superprism effect using a photonic crystal with parallelogram lattice

Damien Bernier, Eric Cassan, Guillaume Maire, Delphine Marris-Morini, Laurent Vivien
Institut d'Electronique Fondamentale, UMR 8622, Bât. 220, Université Paris Sud, 91405 Orsay Cedex, France
Corresponding author: damien.bernier@ief.u-psud.fr

Abstract: *A photonic crystal with parallelogram lattice exhibiting both self collimation and superprism effect for a limited frequency range is studied. The input Gaussian beam shape broadening is limited so that division of a few wavelengths can be achieved without diffraction compensation. Simulations show that a good transmission is obtained without matching stages at the photonic crystal's interface.*

Introduction

Photonic crystals (PC) have attracted much interest for their optical tunable properties in both propagating and bandgap domains. In particular, two-dimensional (2D) slab PCs have been widely investigated for their diffraction properties outside of the photonic bandgap. The band engineering of those PCs has led to the demonstration of structures allowing collimation, focusing or strong wavelength-dependant dispersion [1-5].

Wavelength division using high dispersion has been generally studied for the triangular and square lattice [6]. One of the key problems when using very strong superprism effect is the beam broadening that generally occurs in the same time [7]. Focusing has been proposed to overcome the angular spreading by adding a negative diffraction effect, thus leading to structures with small PC area [8]. A preconditionned region of diffraction compensation is however needed when using this effect. The preconditionned region can be a homogeneous medium if the PC has negative diffraction, but the area needed in this case is large. A second PC with strong diffraction might also be used to obtain a smaller whole structure.

In the present work, another approach is studied to control the beam quality profile in strong superprism dispersive configurations. To avoid beam broadening, PCs bands simultaneously presenting strong dispersion with collimation effect have been investigated.

Such regions are present in square PC lattice geometries. By changing the lattice into a parallelogram one, those regions can be extended and excited by a smaller incident angle. This paper is organized as follows. The diffraction properties of a parallelogram lattice PC are first presented. Beam propagation has then been studied by an effective index propagation method and by Finite-Difference Time-Domain (FDTD) calculations to evaluate the structure resolution and transmission.

Diffraction properties of parallelogram lattice PC

Figure 1 shows the considered photonic crystal. It consists of a parallelogram lattice ($a=300$ nm) of air holes etched within a 220 nm thick dielectric silicon film, with a buried silicon oxide layer of 1 μm and air as top cladding. The lattice vectors have an equal length and are angularly spaced by 105° . The radius r of the holes is $0.3a$. The interface between the homogeneous medium and the PC is along a lattice vector direction of the crystal.

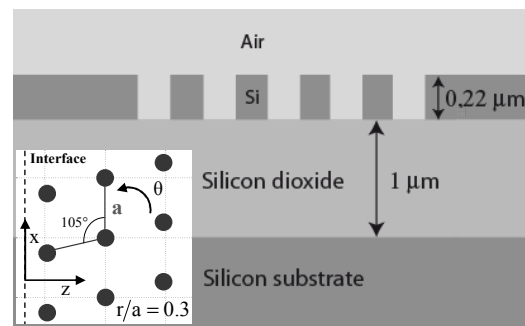


Fig. 1: Considered photonic crystal and interface orientation and SOI slab waveguide structure.

Three-dimensional plane wave (3D-PWM) calculations with a supercell in the vertical direction have been performed using the MIT program [9] to obtain the band structure of the PC. The considered silicon and silica indices at $\lambda=1520$ nm are 3.478 and 1.444, respectively. Figure 2 shows the first band equi-frequency curves of the PC. Wavevectors k_{\parallel} and k_z are the tangential and normal components with respect to the PC interface. Shaded regions are added to exhibit the zones of the reciprocal space with low beam broadening (light gray) and high dispersion (medium gray). Regions presenting both high dispersion and low beam broadening are reported in dark gray. Those zones have been delimited using the divergence p and dispersion q factors previously introduced by Baba et al. to evaluate the superprism resolution [7]. These factors correspond to the variations of the refraction angle with the incident angle and with the normalized frequency, respectively: $p = \partial\theta_r / \partial\theta_{in}$ and $q = \partial\theta_r / \partial(a/\lambda)$. Shaded low beam broadening regions correspond to $|p| < 2$ and strong dispersion areas have been chosen to correspond to $|q| > 35$. For both cases, only modes that propagate within the PC are considered ($|\theta_r| < 90^\circ$). The $\theta_{in} = -50^\circ$ equi-frequency curve is reported in figure 2. For this incidence angle, a frequency domain is found to have low beam broadening and strong dispersion.

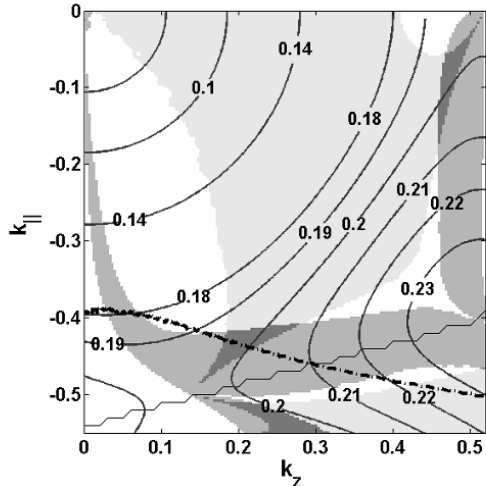


Fig. 2: First band equi-frequency curves of the PC. Equi-incident angle curve for $\theta_N = -50^\circ$ (thick dashed line). Low beam broadening regions (soft gray), strong dispersion regions (medium gray) and areas with both properties are reported (dark gray).

Figure 3 shows the $|p|$ (circle markers) and q (plain square markers) factors along the -50° equi-frequency curve as a function of the wavelength. The p factor value is less than 1 for a 23 nm wavelength range. This corresponds to a beam spreading lower than the one of the homogeneous slab waveguide. Collimation ($p=0$) occurs for $\lambda=1510$ nm with a q factor of 65 that corresponds to $0.49^\circ/\text{nm}$. The p factor is positive for wavelengths above $\lambda=1510$ nm and negative below.

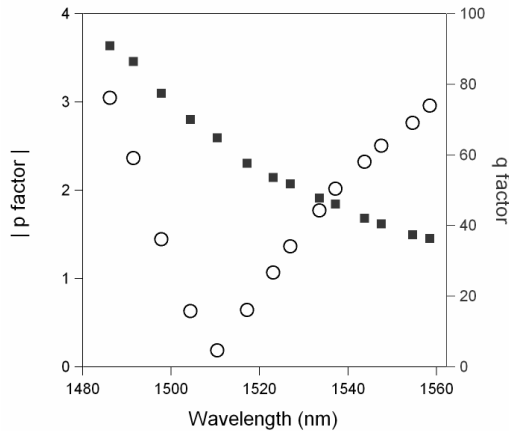


Fig. 3: p (circle markers) and q (square markers) factors around the collimation point for the $\theta_m = -50^\circ$ equi-frequency curve.

Propagation results

To study the PC demultiplexing efficiency, beam propagation method using a method of effective index model has been used [10]. The equi-frequency curves of the planar waveguide and PC have been approximated by second order polynomial functions. The input Gaussian beam has been expanded in plane waves by Fourier transforming along a wavevector

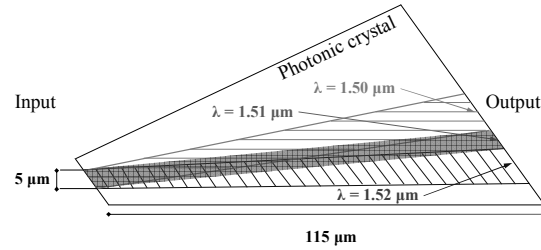


Fig. 4: Gaussian beam propagation using effective index model for $\lambda = 1.50 \mu\text{m}$, $1.51 \mu\text{m}$ and $1.52 \mu\text{m}$ with $5 \mu\text{m}$ wide input beams.

axis parallel to the PC interfaces. The spatial beam shape at a given propagation length has then been calculated by propagating the plane waves using the approximated equi-frequency curves and by inverse Fourier transform, i.e. the high spatial frequency modulation induced by PC holes is not considered.

Starting with a gaussian beam $5 \mu\text{m}$ wide (field $1/e$ width), the length of PC needed to separate beams of $\Delta\lambda=10$ nm around $\lambda=1.51 \mu\text{m}$ has been evaluated. Figure 4 shows the beam width within the PC for $\lambda=1.50 \mu\text{m}$, $\lambda=1.51 \mu\text{m}$, and $\lambda=1.52 \mu\text{m}$. The three beams are separated with a PC propagation length around $115 \mu\text{m}$, leading to a PC area less than $2500 \mu\text{m}^2$.

In order to evaluate the diffraction properties and transmission of the structure, 3D-FDTD simulations have been performed using crystalwave software [11]. The PC being too large to be entirely simulated, only $40 \mu\text{m}$ of PC has been considered. The PC's output interface with the slab planar waveguide has been taken parallel to the input interface. A Gaussian excitor is placed in the silicon film $8 \mu\text{m}$ before the PC interface, and parallel sensors are placed in the homogeneous silicon film before and after the PC. The last one is placed $57 \mu\text{m}$ after the Gaussian excitor so that the beam experiences a $17 \mu\text{m}$ long propagation in the homogeneous medium. Figure 5 shows the simulation settings and beam intensity for $\lambda=1.51 \mu\text{m}$.

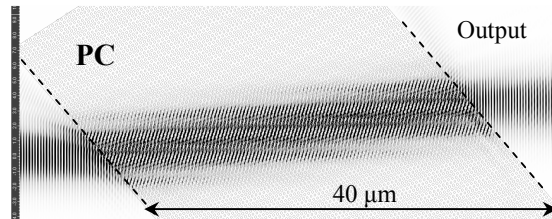


Fig. 5: Beam intensity of 3D-FDTD simulation for $\lambda=1.51 \mu\text{m}$ and an initial beam width of $5 \mu\text{m}$.

The transmission and beam width at the output sensor $W_{\text{FDTD OUT}}$ are resumed on table 1 for $\lambda=1.50 \mu\text{m}$, $1.51 \mu\text{m}$ and $1.52 \mu\text{m}$. The output beam shapes being very close to Gaussian curves, their widths have been obtained by Gaussian fitting. The theoretical beam width after propagation within $57 \mu\text{m}$ in the Si slab waveguide W_{SLAB} is given for comparison (effective

Table 1: FDTD output beam widths and transmissions after a 57 μm propagation (with 40 μm of PC) of a 5 μm input Gaussian beam. Refraction angle θ_R within PC. Theoretical beam width for the homogeneous slab waveguide W_{SLAB} .

	Wavelength		
	1500 nm	1510 nm	1520 nm
$W_{\text{FDTD OUT}}$	5.10 μm	6.24 μm	7.66 μm
Transmission	75.4%	83.9%	90.1%
W_{SLAB}	9.11 μm	9.16 μm	9.22 μm
θ_R	39.51°	44.40°	48.62°

index: 2.854 at $\lambda=1.51 \mu\text{m}$). For the considered wavelengths, the beam width with the PC wavelength-dispersive region is narrower than the width of the beams propagated in the slab homogeneous medium. For $\lambda=1.50 \mu\text{m}$, the output beam is 5.10 μm wide that is almost equal to the initial 5.0 μm width. For this wavelength, the beam propagates within the PC with a negative p value that compensates the broadening of the beam within the 17 μm long homogeneous slab. The collimation wavelength found by FDTD calculations is close to 1505 nm, i.e. close to 1510 nm expected from plane wave method calculations.

The dispersion has also been evaluated by FDTD using the central beam position at the output sensor. The refraction angles are 39.51°, 44.40° and 48.62° for $\lambda=1.50 \mu\text{m}$, 1.51 μm and 1.52 μm , respectively. The dispersion at the FDTD collimation point ($\lambda=1505 \text{ nm}$) is then 0.49°/nm that agrees with the q factor given by plane wave expansion calculations at collimation point.

The transmission of the PC has been evaluated using the positive flux recorded by sensors before and after the PC, both normal to the beam's direction of propagation. A transmission from 75.4 % to 90.1% is found as the wavelength goes from 1500 nm to 1520 nm. Losses are mainly due to the input and output interface mismatching and increases as the wavelength shorten. Losses for wavelengths below 1500 nm become important as the excited Bloch waves are close to the edge of the first Brillouin zone.

Given the high dispersion parameter for wavelength above 1520 nm and below 1500 nm, this structure can be used to divide other wavelengths provided the enlargement of the wavelength channel spacing. To keep a $\Delta\lambda$ at 10 nm for a larger wavelength range, a precompensation PC that has an opposite wavelength dependant p factor might be used to keep the beam width at its minimum along the output interface.

Conclusion

A photonic crystal exhibiting both strong dispersion and collimation effect has been studied. Simulations showed low beam distortion for Gaussian beams 5 μm wide with a mean transmission around 83%

without matching stages at the PC interfaces. This single PC structure can divide three wavelengths spaced by 10 nm using an area lower than 2500 μm^2 without beam preconditioning regions. The PC structure might be further optimized to enlarge the wavelength range of low beam broadening.

Acknowledgments

The authors would like to acknowledge Suzanne Laval for fruitful discussions.

References

- 1 T. Matsumoto et al, Optics Express 13, 10768-10766 (2005).
- 2 H. Kosaka et al, J. Lightwave Technol, vol. 17, no. 11, 2032-2038, November 1999.
- 3 L. Wu et al, IEEE J. Quantum Electron., 38, 915-918 (2002).
- 4 S.N. Tandon et al, Photonic and Nanostructures, Fundamentals and Applications 3 (2005) 10–18
- 5 A. Lupu et al, Optics Express 12, 5690-5696 (2004).
- 6 B. Momeni et al, J. Select. Areas Commun. 23, 1355-1364 (2005).
- 7 T. Baba et al, Appl. Phys. Lett. 81, 2325-2327 (2002).
- 8 B. Momeni et al, Optics Express 14 No 6, 2413-2422 (2006).
- 9 MIT photonic band (MPB) available at: <http://ab-initio.mit.edu/photons/>
- 10 B. Momeni et al, J. Lightwave Technol., vol. 23, no. 3, pp. 1522–1532, Mar. 2005.
- 11 Lavrinenko et al, "CrystalWave", Photon Design, www.photond.com